

The C-terminal Domain Revealed in the Structure of RNA Polymerase II

Gavin D. Meredith¹, Wei-Hau Chang¹, Yang Li¹, David A. Bushnell¹
Seth A. Darst² and Roger D. Kornberg^{1*}

¹*Department of Structural Biology, Stanford University School of Medicine, Stanford CA 94305-5400, USA*

²*The Rockefeller University Box 224, 1230 York Avenue, New York, NY 10021-6399 USA*

The location of the CTD in the structure of RNA polymerase II has been determined by electron crystallography at 16 Å resolution. Difference maps between wild-type enzyme and that lacking the CTD, or with an antibody fragment bound in place of the CTD, disclose the site of attachment of the CTD to the polymerase. Appropriate display of the polymerase structure reveals the CTD as an element projecting from this site of attachment into solution. A low relative density and large volume of this element identify the CTD as a conformationally mobile region.

© 1996 Academic Press Limited

Keywords: RNA polymerase II; CTD; structure; electron crystallography; transcription

*Corresponding author

Introduction

The C-terminal domain (CTD) of the largest subunit of RNA polymerase II (pol II) contains a seven-amino acid motif, tandemly repeated 27 times in yeast and 52 in man, with a consensus sequence (Tyr-Ser-Pro-Ser-Thr-Pro-Ser) that is highly conserved across species (Corden, 1990). Unique to pol II, the CTD is essential for cell viability and plays a central role in the regulation of mRNA synthesis *in vivo*. The CTD is also required for initiation of transcription and for the response to activator proteins at some promoters *in vitro* (Thompson *et al.*, 1989; Lee & Greenleaf, 1991; Kang & Dahmus, 1993; Buermeier *et al.*, 1995; Gerber *et al.*, 1995). While mechanisms have not been established, there is biochemical and genetic evidence for the involvement of many CTD-interacting proteins in transcription (Conaway *et al.*, 1992; Koleske *et al.*, 1992; Usheva *et al.*, 1992; Serizawa *et al.*, 1993; Thompson *et al.*, 1993; Kim *et al.*, 1994; Maxon *et al.*, 1994; Yuryev & Corden, 1994).

The CTD undergoes a cycle of extensive phosphorylation and dephosphorylation at every round of transcription initiation, and the murine CTD is also glycosylated (Kelly *et al.*, 1993; Zawel *et al.*, 1993; Dahmus, 1995). Serine, threonine and tyrosine residues in the CTD are all targets of phosphorylation, and a number of kinases capable of these modifications, as well as a CTD-specific

phosphatase, have been described (Feaver *et al.*, 1991; Lee & Greenleaf, 1991; Zhang & Corden, 1991a; Lu *et al.*, 1992; Baskaran *et al.*, 1993; Dvir *et al.*, 1993; Chambers & Dahmus, 1994; Svejstrup *et al.*, 1994). Purified preparations of pol II contain relatively unphosphorylated and hyperphosphorylated forms, denoted I_a and I_o, respectively. There are many indications that the I_a form is favored for entry into preinitiation complexes, while the I_o form is associated primarily with elongation complexes (Lu *et al.*, 1991; Chesnut *et al.*, 1992; Greenleaf, 1993; Kang & Dahmus, 1993; O'Brien *et al.*, 1994). Phosphorylation has been suggested to alter either the conformation of the CTD or its affinity for other components of the transcriptional machinery.

The structure of the CTD has proved difficult to establish. NMR and circular dichroism studies of a synthetic peptide containing eight repeats of the consensus sequence (Cagas & Corden, 1995), the minimum number required for viability of yeast (Nonet *et al.*, 1987; West & Corden, 1995), suggested an extended conformation with successive beta turns and apparent right-handed helical symmetry. Similar results were obtained from circular dichroism studies of synthetic peptides containing either one or approximately 83 to 97 consensus repeats, but in this case a left-handed helical structure was proposed (Nishi *et al.*, 1995). Yet additional structures have been put forward based on modeling (Matsushima *et al.*, 1990; Suzuki, 1990). Finally, an increase in the apparent Stokes radius of bacterially expressed murine CTD upon phosphorylation by a purified kinase points to a more

Abbreviations used: CTD, C-terminal domain; pol II, polymerase II; 2-D, two-dimensional; 3-D, three-dimensional.

extended conformation following modification (Zhang & Corden, 1991b).

The three-dimensional (3-D) structure of yeast RNA polymerase II in form IIa has been determined by electron crystallography of 2-D crystals in negative stain at 16 Å resolution (Darst *et al.*, 1991a). Notable features of the structure include a 25 Å channel, thought to bind duplex DNA, and a finger-like extension having about 75% of the volume expected for a globular domain with the mass of the CTD. We report here on the location and conformation of the CTD in this polymerase structure.

Results

A mutant strain of yeast was constructed with a 12CA5 monoclonal antibody recognition site and two factor Xa protease cleavage sites interposed between the CTD and the rest of the largest polymerase subunit (Niman *et al.*, 1983; Wilson *et al.*, 1984; Li & Kornberg, 1994). Factor Xa cleavage of the purified enzyme yielded a CTD-less polymerase, with activity that was indistinguishable from that of the intact molecule in transcription reconstituted with purified proteins *in vitro* (Li & Kornberg, 1994). The strain was further modified for removal of pol II subunits 4 and 7, shown previously to facilitate crystallization (Edwards *et al.*, 1991). Enzyme isolated from this strain (YLC2Δ4) and cleaved with factor Xa (CTD-less Δ4/7 pol II) formed 2-D crystals isomorphous with those of intact Δ4/7 pol II, allowing difference Fourier analysis.

As previously reported, a unit cell of the 2-D crystals contained a central pair of enzyme molecules, related by an apparent dyad between the molecules in the plane of the crystal (Figure 1a; Darst *et al.*, 1991b). In view of slight differences between these two molecules in negative stain, we preferred to perform image processing in plane group *p*1. Ten electron micrographs of both CTD-less Δ4/7 pol II and Δ4/7 pol II crystals in projection were subjected to image processing, averaging of Fourier components, and Fourier synthesis. Both data sets were complete to 15.7 Å resolution, and the resulting electron density maps were essentially the same as those previously obtained (Darst *et al.*, 1991a,b). A Fourier difference map between the two data sets (Figure 1b) contained appreciable density at many sites. Statistical analysis allowed some discrimination amongst these sites. The micrographs were individually subjected to image processing and Fourier synthesis, yielding two sets of electron density maps, which were compared pixel-by-pixel with the use of a Student's *t*-test where variances were not assumed to be equal (Milligan & Flicker, 1987; Mendenhall & Sincich, 1988). The resulting statistical significance map, contoured at the 99.95% confidence level (Figure 1c), contained peaks along one edge of the polymerase molecule and at one intermolecular contact. These peaks were apparently real, since they did not appear upon splitting

a set of electron density maps in two and computing statistical significance maps between the half sets (data not shown). These results are inconclusive, since there are multiple peaks, most smaller than the diameter of about 30 Å expected for a globular domain having the mass of the CTD.

More definitive evidence was obtained through binding of a 12CA5 antibody fragment. In the mutant pol II described above, an epitope for antibody binding was located at the C terminus of the largest subunit following factor Xa cleavage for removal of the CTD. A large excess of anti-epitope Fab was added to the CTD-less enzyme (epi-CTD-less Δ4/7 pol II) prior to crystallization. Large, well-ordered 2-D crystals were less abundant in the presence of Fab, but were isomorphous with those obtained in its absence. Five images were processed and averaged, yielding data complete to 20.0 Å resolution. A Fourier difference map (Figure 1d) between these data and those described above for the CTD-less enzyme, truncated to 20.0 Å, contained a major, ellipsoidal density along the edge of one molecule, a lesser density in the same location on the apparent dyad-related molecule, and small peaks near the 25 Å channel of one of the molecules. A statistical difference map, contoured at the 99.95% confidence level (Figure 1e), contained the major, ellipsoidal density and peaks near the 25 Å channel. The shape and dimensions of the ellipsoidal density were in good agreement with those of an Fab in negative stain (Boisset *et al.*, 1993; Smith *et al.*, 1993). The location of this density corresponded with that of the peaks along the lower edge of a polymerase molecule in the difference map between intact and CTD-less enzymes (Figure 1c).

As a control, intact Δ4/7 pol II (lacking an epitope tag) was crystallized in the presence of anti-epitope Fab. Six images were processed and averaged, and data to 20.0 Å resolution were subtracted from that of the cocrystal of Fab with epi-CTD-less Δ4/7 pol II described above. Any contribution arising from non-specific Fab binding should be removed in this way. While the resulting Fourier difference map (Figure 1f) still exhibited extraneous density, a statistical significance map (Figure 1g) contained only peaks in the location of the Fab and, to a lesser extent, in the corresponding location on the apparent dyad-related polymerase molecule. Peaks in the vicinity of the 25 Å channel were eliminated. The density in the location of the Fab may have appeared fragmented because data for intact polymerase were subtracted from that for CTD-less enzyme, resulting in a negative contribution from the CTD. In support of this possibility, adding back the CTD by superposition of statistical significance maps reconnected the fragmented density and filled out the profile of the Fab (Figure 1h). Two types of experiment, removal of the CTD and binding of Fab, thus gave consistent results and pointed to a region on the surface of the polymerase from which the CTD likely extends into solution.

Inasmuch as the difference between intact and CTD-less polymerases failed to reveal a single

contiguous region of the size expected, the CTD must possess a degree of conformation mobility. We therefore examined the previously determined 3-D density map for comparatively weak features, by contouring at lower levels in space group *P1*. On reducing the contour level only slightly, from 1.8 to 1.0 standard deviations above the average, a new density appeared in the location of the CTD (Figure 2). Remarkably, there was no other significant new feature at the lower contour level. The

new density was connected to the body of the polymerase by a slender neck that coincided with the location of one end of a bound Fab as seen in projection (Figure 1e), consistent with an epitope at the base of the CTD interacting with the tip of the Fab. The new density appeared flattened against a surface parallel to the plane of the crystal (possibly either the lipid layer on which the crystal was grown or the carbon film on which it was deposited, although the orientation of the crystal with respect

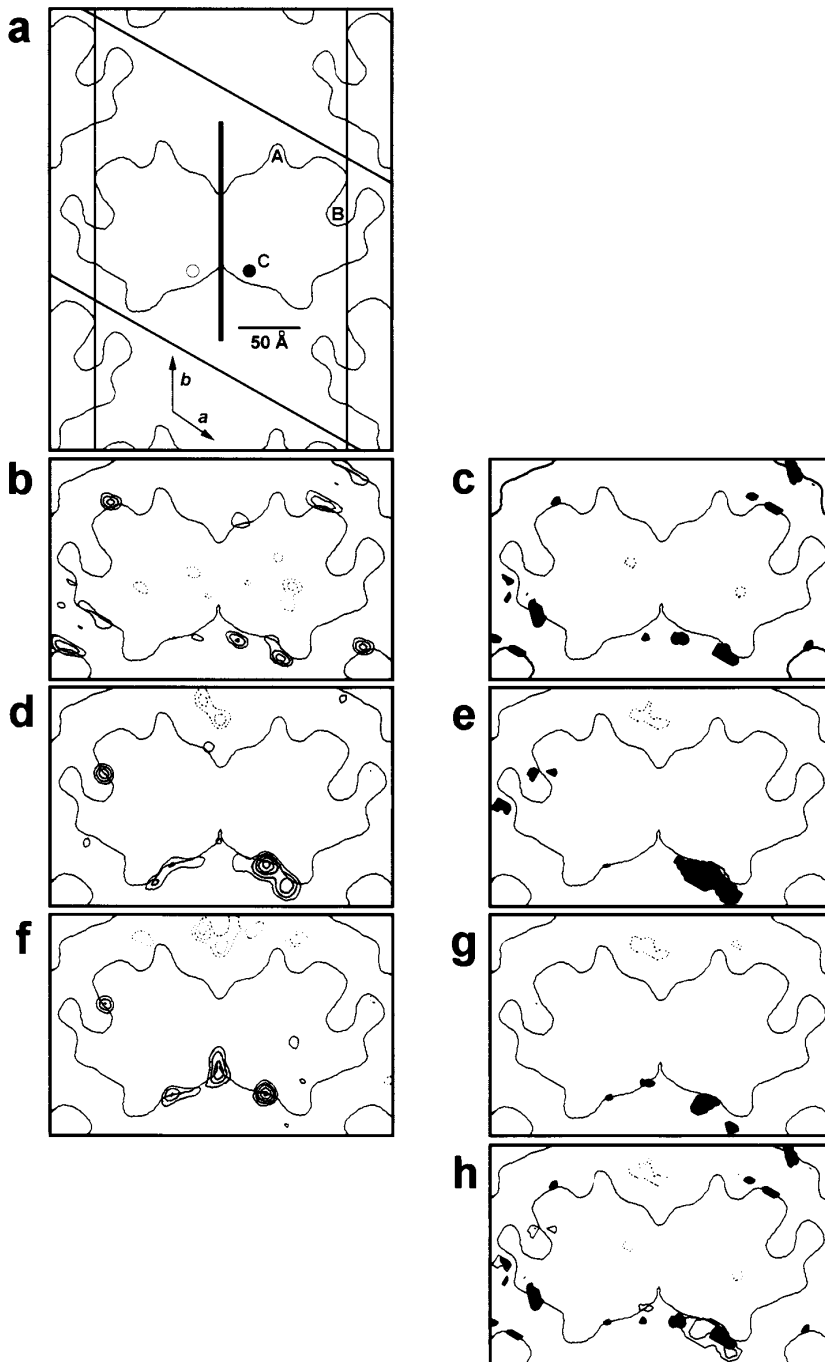


Figure 1. Projection maps of yeast RNA polymerase II and of differences due to deletion of the CTD or to Fab association with an epitope at the base of the CTD. a, Outlines of CTD-less $\Delta 4/7$ pol II molecules in 2-D crystals. The two polymerase molecules in the center of the *p1* unit cell indicated ($a = 234 \pm 2 \text{ \AA}$, $b = 231 \pm 2 \text{ \AA}$, $\gamma = 120 \pm 0.5^\circ$) are related by an apparent dyad axis in the plane of the crystal (heavy vertical line). Features noted: A, a finger-like extension, previously suggested to be due to the CTD (Darst *et al.*, 1991a); B, a channel about 25 \AA in diameter, suggested to bind duplex DNA (Darst *et al.*, 1991a); and C, approximate sites of attachment of the CTD determined in this work, symbolized by open and filled circles for density extending into and out of the page respectively. b, Fourier difference map between average images of $\Delta 4/7$ pol II crystals and CTD-less $\Delta 4/7$ pol II crystals. c, Statistical significance map of the difference in b. d, Fourier difference map between average images of Fab:epi-CTD-less $\Delta 4/7$ pol II cocrystals and CTD-less $\Delta 4/7$ pol II crystals. e, Statistical significance map of the difference in d. f, Fourier difference map between average images of Fab:epi-CTD-less $\Delta 4/7$ pol II cocrystals and Fab:intact $\Delta 4/7$ pol II cocrystals. g, Statistical significance map of the difference in f. h, Superposition of the statistically significant positive peaks in c (in black), e (in white), and g (in grey) on the molecular outlines in a; the negative peaks are indicated by broken lines. In b, d, and f, differences in projection 2.0 standard deviations and greater above the average, contoured at steps of 0.5 standard deviations, are shown in grey, superimposed on the molecular outlines in a. Differences 2.0 standard deviations below the average, contoured at the same step size,

are indicated by broken lines. In c, e, and g, positive significance peaks at the 99.95% confidence level, determined by pixel-by-pixel application of a two-sided Student's *t*-test, are shown in black superimposed on the molecular outlines in a, while negative peaks are indicated by broken lines. Details of average images are given in Table 1.

Table 1. Details of averaged datasets

Dataset	No. of images	No. of molecules	Average phase error (°)	Resolution (Å)	No. of reflections ^a
Intact CTD Δ4/7 pol II	10	18,000	20.6	15.7	286/294
CTD-less Δ4/7 pol II	10	46,000	24.7	15.7	286/294
Fab:epi-CTD-less Δ4/7 pol II cocrystals	5	7500	25.4	20.0	172/185
Fab:Δ4/7 pol II cocrystals	6	21,000	20.3	15.7	283/294

^a Number of reflections with a signal to noise ratio greater than one observed over the number of reflections possible within the stated resolution limit.

to the supporting surface is unknown). This density occupied a volume about four times that expected from the mass of the CTD and may therefore represent multiple conformations of the CTD, constrained by interaction with or by steric hindrance due to an adjacent planar surface. The lack of a corresponding density on the apparent dyad-related polymerase molecule may reflect a

lack of constraint on a CTD extending in the opposite direction, relative to the plane of the crystal. In the projection maps of Fab cocrystals described above, one of the apparent dyad-related polymerase molecules failed to display associated Fab density. Fab may have been present, bound at the site of attachment of the CTD to this molecule, but not uniquely oriented due to flexibility of the residues immediately preceding the CTD, and so not revealed at the contour level used. That there is flexibility in this region of the largest subunit of pol II is consistent with previous molecular genetic studies showing a tolerance to insertions in this region *in vivo* (Li & Kornberg, 1994).

Discussion

These results rule out the previous suggestion that a finger-like extension from the polymerase structure noted above (Figure 1a) might be due to the CTD (Darst *et al.*, 1991a). This extension is unaffected by removal of the CTD (Figure 1b,c) and the site of attachment of the CTD demonstrated here is on the opposite side of the polymerase molecule. The location of the CTD is further of interest because it identifies a region of the polymerase structure occupied by the largest subunit, Rpb1. The site of attachment of the CTD is the C terminus of Rpb1 of the CTD-less enzyme, and the 25 Å channel noted above (Figure 1a) is also likely formed, at least in part, by Rpb1 (Allison *et al.*, 1985; Sweetser *et al.*, 1987; Darst *et al.*, 1991a), defining two boundaries of this subunit within the structure.

In view of the several lines of evidence presented here for conformational mobility of the CTD, the appearance of density due to this domain in the 3-D structure was fortunate, probably owing to the lipid layer crystallization procedure and preservation in negative stain. The CTD is evidently so mobile and unstructured as to be fully penetrated by stain when not constrained against a surface. This is consistent with recent results from NMR and circular dichroism studies of synthetic CTDs mentioned above (Cagas & Corden, 1995; Nishi *et al.*, 1995). Further, an Fab bound at the base of the CTD appeared to be barely visible in the absence of a surface constraint, suggesting that the point of attachment of the CTD to the body of the

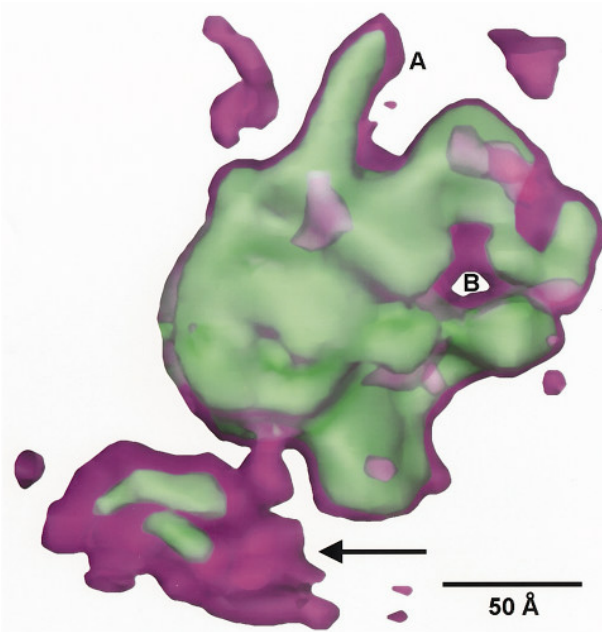


Figure 2. Three-dimensional model of Δ4/7 RNA polymerase II showing the CTD. The protein surface from electron crystallography in negative stain, processed as space group *P1*, contoured at 1.8 standard deviations above the average density (Darst *et al.*, 1991a), is shown in green, while results of contouring the same data at 1.0 standard deviations above the average are in purple. The right-most molecule of an apparent dyad pair is viewed here following rotation 6° around the vertical axis (*b*) in Figure 1a and 18° around the horizontal axis (perpendicular to the *b* axis in the plane of crystallization). The finger-like projection, A, and the 25 Å channel, B, of Figure 1a are labelled. Density due to the CTD is indicated by an arrow. The image was generated with the program package SYNU (Hessler *et al.*, 1992) and edited to remove extraneous density from neighboring Δ4/7 pol II molecules with the program Adobe Photoshop 3.0.

polymerase molecule is flexible as well. Deletions or substitutions in the sequence immediately preceding the CTD may shed light on the importance of such flexibility for polymerase function.

The results presented here form a basis for comparison with modified forms of the domain and its association with other molecules. The analysis may be repeated with the CTD in a hyperphosphorylated state, suggested to induce a more extended conformation of the domain. Future studies may also be directed towards cocrystals with CTD-binding proteins, such as kinases (Cisek & Corden, 1989; Payne *et al.*, 1989; Lee & Greenleaf, 1991; Stone & Reinberg, 1992; Baskaran *et al.*, 1993; Dvir *et al.*, 1993; Feaver *et al.*, 1994; Liao *et al.*, 1995), phosphatases (Chambers & Dahmus, 1994), and a multiprotein mediator complex whose interaction with the CTD is necessary for both activation and repression of transcription (Kim *et al.*, 1994; Li *et al.*, 1995).

Materials and Methods

Plasmids and strains

Plasmid pSPL8 was constructed by insertion of a 2.9 kb *EcoRV/SalI* genomic fragment from pRP41 that contained the entire *RPB4* coding sequence into *EcoRV/XhoI* sites of pSP73 (Promega) (Woychik & Young, 1989). The 1.6 kb *PvuII/SpeI* fragment of pSPL8 containing the majority of the *RPB4* coding sequence was replaced by a 3.81 kb *XbaI/BamHI* fragment containing a *hisG-URA3-hisG* insert (Alani *et al.*, 1987) from pSPK/O (derived from pSP73, a gift from Brad Cairns) to give pSPL9. For this purpose, pSPK/O was digested with *BamHI*, followed by treatment with DNA polymerase I large fragment to fill in the ends, and digestion with *XbaI*. Plasmid pSPL9 was digested with *BamHI* and used to transform *Saccharomyces cerevisiae* strain YLC2 (*MATa ura3-52 leu2-3 leu2-112 his3-Δ300 rpb1-187::HIS3/[YCpL14 (LEU2 CEN4 RPB1-epi2FXa)]*) by the method of Rothstein to yield strain YLC2Δ4 (*MATa ura3-52 leu2-3 leu2-112 his3-Δ300 rpb1-187::HIS3 rpb4Δ1::URA3/[YCpL14 (LEU2 CEN4 RPB1-epi2FXa)]*) (Rothstein, 1983; Li & Kornberg, 1994). The replacement of the genomic *RPB4* sequence was confirmed by Southern blot analysis.

IgG purification and Fab preparation

Monoclonal 12CA5 IgG was purified from murine ascites (Babco) on Protein A-Sepharose (Sigma) following precipitation with 50% ammonium sulfate. Fabs were obtained by elastase (Boehringer Mannheim) cleavage of mAb 12CA5 followed by separation from uncleaved IgG and residual Fc fragments on Protein A-Sepharose as described for murine isotype 2b IgG (Parham, 1983).

Specimen preparation

RNA polymerases, prepared as described (Edwards *et al.*, 1990; Li & Kornberg, 1994) were crystallized on lipid layers (Darst *et al.*, 1991b) in nylon wells (Asturias & Kornberg, 1995) from solutions containing 70 to 100 μg protein/ml, 50 mM Tris-HCl (pH 7.5), 60 mM (NH₄)₂SO₄, 10% (v/v) glycerol, 5 mM spermidine, 5 mM dithiothreitol under argon on a motion-free table for 8 to 12 hours at 4°C. Where Fabs were used, they were added in 45-fold

molar excess over RNA polymerase at a reduced dithiothreitol concentration of 1 mM and allowed to bind for 45 minutes at room temperature, followed by one hour at 4°C, prior to crystallization. Crystals were transferred to glow-discharged carbon-coated 400 mesh electron microscope grids, washed with 0.05% (v/v) Tween-20, washed with water, and stained with 1% (w/v) uranyl acetate as described (Asturias & Kornberg, 1995).

Electron microscopy and image processing

Images were recorded on a Philips EM400T with a 100 kV accelerating voltage under low dose conditions (<10 electrons per Å²) at a magnification of 37,300× on Kodak SO163 film. A defocus of about 3000 Å yielded images with a contrast transfer function with its first zero corresponding to about 10 Å resolution. Suitable images were selected by optical diffractometry, digitized with a Perkin Elmer scanning microdensitometer at 20 μm square pixel-size, and processed by standard methods (Amos *et al.*, 1982; Henderson *et al.*, 1986; Darst *et al.*, 1991b).

Difference calculation and statistical analysis

Scaled Fourier differences were calculated as described (Kubalek *et al.*, 1987). Significance maps were calculated with a Student's *t*-test statistic (Milligan & Flicker, 1987) modified for small sample size where population variances were not assumed to be equal (Mendenhall & Sincich, 1988).

Acknowledgements

G.D.M. is a National Science Foundation (NSF) Fellow and was supported in part by the National Institutes of Health (NIH) Molecular Biology Training Program. S.A.D. is a Lucille P. Markey Scholar. This research was supported by a grant from the Lucille P. Markey Charitable Trust, NIH grant AI21144 to R.D.K. and by the Human Frontiers Science Program.

References

- Alani, E., Cao, L. & Kleckner, N. (1987). A method for gene disruption that allows repeated use of *URA3* selection in the construction of multiply disrupted yeast strains. *Genetics*, **116**, 541–545.
- Allison, L. A., Moyle, M., Shales, M. & Ingles, C. J. (1985). Extensive homology among the largest subunits of eukaryotic and prokaryotic RNA polymerases. *Cell*, **42**, 599–610.
- Amos, L. A., Henderson, R. & Unwin, P. N. T. (1982). Three-dimensional structure determination by electron microscopy of two-dimensional crystals. *Prog. Biophys. Mol. Biol.* **39**, 183–231.
- Asturias, F. J. & Kornberg, R. D. (1995). A novel method for transfer of two-dimensional crystals from the air/water interface to specimen grids. *J. Struct. Biol.* **114**, 60–66.
- Baskaran, H., Dahmus, M. E. & Wang, J. Y. J. (1993). Tyrosine phosphorylation of mammalian RNA polymerase II carboxyl-terminal domain. *Proc. Natl Acad. Sci. USA*, **90**, 11167–11171.
- Boisset, N., Radermacher, M., Grassucci, R., Traveau, J.-C., Liu, W., Lamy, J., Frank, J. & Lamy, J. N. (1993). Three-dimensional immunoelectron microscopy of

- scorpion hemocyanin labeled with a monoclonal Fab fragment. *J. Struct. Biol.* **111**, 234–244.
- Buermeyer, A. B., Strasheim, L. A., McMahon, S. L. & Farnham, P. J. (1995). Identification of *cis*-acting elements that can obviate a requirement for the C-terminal domain of RNA polymerase II. *J. Biol. Chem.* **270**, 6798–6807.
- Cagas, P. M. & Corden, J. L. (1995). Structural studies of a synthetic peptide derived from the carboxyl-terminal domain of RNA polymerase II. *Proteins: Struct. Funct. Genet.* **21**, 149–160.
- Chambers, R. S. & Dahmus, M. E. (1994). Purification and characterization of a phosphatase from HeLa cells which dephosphorylates the C-terminal domain of RNA polymerase II. *J. Biol. Chem.* **269**, 26243–26248.
- Chesnut, J. D., Stephens, J. H. & Dahmus, M. E. (1992). The interaction of RNA polymerase II with the Adenovirus-2 major late promoter is precluded by phosphorylation of the C-terminal domain of subunit IIa. *J. Biol. Chem.* **267**, 10500–10506.
- Cisek, L. J. & Corden, J. L. (1989). Phosphorylation of RNA polymerase by the murine homologue of the cell-cycle control protein cdc2. *Nature*, **339**, 679–684.
- Conaway, R. C., Bradsher, J. N. & Conaway, J. W. (1992). Mechanism of assembly of the RNA polymerase II preinitiation complex. *J. Biol. Chem.* **267**, 8464–8467.
- Corden, J. L. (1990). Tails of RNA polymerase II. *Trends Biochem. Sci.* **15**, 383–387.
- Dahmus, M. E. (1995). Phosphorylation of the C-terminal domain of RNA polymerase II. *Biochim. Biophys. Acta*, **1261**, 171–182.
- Darst, S. A., Edwards, A. M., Kubalek, E. W. & Kornberg, R. D. (1991a). Three-dimensional structure of yeast RNA polymerase II at 16 Å resolution. *Cell*, **66**, 121–128.
- Darst, S. A., Kubalek, E. W., Edwards, A. M. & Kornberg, R. D. (1991b). Two-dimensional and epitaxial crystallization of a mutant form of yeast RNA polymerase II. *J. Mol. Biol.* **221**, 347–357.
- Dvir, A., Stein, L. Y., Calore, B. L. & Dynan, W. S. (1993). Purification and characterization of a template-associated protein kinase that phosphorylates RNA polymerase II. *J. Biol. Chem.* **268**, 10440–10447.
- Edwards, A. M., Darst, S. A., Feaver, W. J., Thompson, N. E., Burgess, R. R. & Kornberg, R. D. (1990). Purification and lipid-layer crystallization of yeast RNA polymerase II. *Proc. Natl Acad. Sci. USA*, **87**, 2122–2126.
- Edwards, A. M., Kane, C. M., Young, R. A. & Kornberg, R. D. (1991). Two dissociable subunits of yeast RNA polymerase II stimulate the initiation of transcription at a promoter *in vitro*. *J. Biol. Chem.* **266**, 71–75.
- Feaver, W. J., Gileadi, O. & Kornberg, R. D. (1991). Purification and characterization of yeast RNA polymerase II transcription factor b. *J. Biol. Chem.* **266**, 19000–19005.
- Feaver, W. J., Svejstrup, J. Q., Henry, N. L. & Kornberg, R. D. (1994). Relationship of CDK-activating kinase and RNA polymerase II CTD kinase TFIIF/TFIIK. *Cell*, **79**, 1103–1109.
- Gerber, H.-P., Hagmann, M., Seipel, K., Georgiev, O., West, M. A. L., Litingtung, Y., Schaffner, W. & Corden, J. L. (1995). RNA polymerase II C-terminal domain required for enhancer-driven transcription. *Nature*, **374**, 660–662.
- Greenleaf, A. L. (1993). A positive addition to a negative tail's tale. *Proc. Natl Acad. Sci. USA*, **90**, 10896–10897.
- Henderson, R., Baldwin, J. M., Downing, K. H., Lepault, J. & Zemlin, F. (1986). Structure of purple membrane from *Halobacterium halobium*: recording, measurement and evaluation of electron micrographs at 3.5 Å resolution. *Ultramicroscopy*, **19**, 147–178.
- Hessler, D., Young, S. J., Carragher, B. O., Martone, M., Lamont, S., Whittaker, M., Milligan, R. A., Masliah, E., Hinshaw, J. E. & Ellisman, M. H. (1992). Programs for visualization in 3-dimensional microscopy. *NeuroImage*, **1**, 55–67.
- Kang, M. E. & Dahmus, M. E. (1993). RNA polymerase IIA and IIO have distinct roles during transcription from the TATA-less murine dihydrofolate reductase promoter. *J. Biol. Chem.* **268**, 25033–25040.
- Kelly, W. G., Dahmus, M. E. & Hart, G. W. (1993). RNA polymerase II is a glycoprotein. *J. Biol. Chem.* **268**, 10416–10424.
- Kim, Y.-J., Bjorklund, S., Li, Y., Sayre, M. H. & Kornberg, R. D. (1994). A multiprotein mediator of transcriptional activation and its interaction with the C-terminal repeat domain of RNA polymerase II. *Cell*, **77**, 599–608.
- Koleske, A. J., Buratowski, S., Nonet, M. & Young, R. A. (1992). A novel transcription factor reveals a functional link between the RNA polymerase II CTD and TFIID. *Cell*, **69**, 883–894.
- Kubalek, E., Ralston, S., Lindstrom, J. & Unwin, N. (1987). Location of subunits within the acetylcholine receptor by electron image analysis of tubular crystals from *Torpedo marmorata*. *J. Cell Biol.* **105**, 9–18.
- Lee, J. M. & Greenleaf, A. L. (1991). CTD kinase large subunit is encoded by CTK1, a gene required for normal growth of *Saccharomyces cerevisiae*. *Gene Exp.* **1**, 149–167.
- Li, Y. & Kornberg, R. D. (1994). Interplay of positive and negative effectors in function of the C-terminal repeat domain of RNA polymerase II. *Proc. Natl Acad. Sci. USA*, **91**, 2362–2366.
- Li, Y., Bjorklund, S., Jiang, Y. W., Kim, Y.-J., Lane, W. S., Stillman, D. J. & Kornberg, R. D. (1995). Yeast global transcriptional regulators Sin4 and Rgr1 are components of mediator complex/RNA polymerase II holoenzyme. *Proc. Natl Acad. Sci. USA*, **92**, 10864–10868.
- Liao, S.-M., Zhang, J., Jeffrey, D. A., Koleske, A. J., Thompson, C. M., Chao, D. M., Viljoen, M., van Vuuren, H. J. J. & Young, R. A. (1995). A kinase-cyclin pair in the RNA polymerase II holoenzyme. *Nature*, **374**, 193–196.
- Lu, H., Flores, O., Weinmann, R. & Reinberg, D. (1991). The nonphosphorylated form of RNA polymerase II preferentially associates with the preinitiation complex. *Proc. Natl Acad. Sci. USA*, **88**, 10004–10008.
- Lu, H., Zawel, L., Fisher, L., Egly, J.-M. & Reinberg, D. (1992). Human general transcription factor IIH phosphorylates the C-terminal domain of RNA polymerase II. *Nature*, **358**, 641–645.
- Matsushima, N., Creutz, C. E. & Kretsinger, R. H. (1990). Polyproline, β-turn helices, novel secondary structures proposed for the tandem repeats within rhodopsin, synaptophysin, synexin, gliadin, RNA polymerase II, hordein, and gluten. *Proteins: Struct. Funct. Genet.* **7**, 125–155.
- Maxon, M. E., Goodrich, J. A. & Tijian, R. (1994). Transcription factor IIE binds preferentially to RNA polymerase IIa and recruits TFIIF: a model for promoter clearance. *Genes Dev.* **8**, 515–524.
- Mendenhall, W. & Sincich, T. (1988). *Statistics for the Engineering and Computer Sciences*, pp. 376–411, Dellen Publishing Company, San Francisco, CA.

- Milligan, R. A. & Flicker, P. F. (1987). Structural relationships of actin, myosin, and tropomyosin revealed by cryo-electron microscopy. *J. Cell Biol.* **105**, 29–39.
- Niman, H. L., Houghten, R. A., Walker, L. E., Reisfeld, R. A., Wilson, I. A., Hogle, J. M. & Lerner, R. A. (1983). Generation of protein-reactive antibodies by short peptides is an event of high frequency: implications for the structural basis of immune recognition. *Proc. Natl Acad. Sci. USA*, **80**, 4949–4953.
- Nishi, N., Ohiso, I., Sakairi, N., Torura, S., Tsunemi, M. & Oka, M. (1995). Synthesis and conformational investigation of tandem repeat sequence in RNA polymerase II. *Biochem. Biophys. Res. Commun.* **206**, 981–987.
- Nonet, M., Sweetser, D. & Young, R. A. (1987). Functional redundancy and structural polymorphism in the largest subunit of RNA polymerase II. *Cell*, **50**, 909–915.
- O'Brien, T., Hardin, S., Greenleaf, A. & Lis, J. T. (1994). Phosphorylation of RNA polymerase II C-terminal domain and transcriptional elongation. *Nature*, **370**, 75–77.
- Parham, P. (1983). On the fragmentation of monoclonal IgG1, IgG2a, and IgG2b from BALB/c mice. *J. Immunol.* **131**, 2895–2902.
- Payne, J. M., Laybourn, P. J. & Dahmus, M. E. (1989). The transition of RNA polymerase II from initiation to elongation is associated with phosphorylation of the carboxyl-terminal domain of subunit I α . *J. Biol. Chem.* **264**, 19621–19629.
- Rothstein, R. J. (1983). One-step gene disruption in yeast. *Methods Enzymol.* **101**, 202–211.
- Serizawa, H., Conaway, J. W. & Conaway, R. C. (1993). Phosphorylation of C-terminal domain of RNA polymerase II is not required in basal transcription. *Nature*, **363**, 371–374.
- Smith, T. J., Olson, N. H., Cheng, R. H., Liu, H., Chase, E. S., Lee, W. M., Leippe, D. M., Mosser, A. G., Rueckert, R. R. & Baker, T. S. (1993). Structure of human rhinovirus complexed with Fab fragments from a neutralizing antibody. *J. Virol.* **67**, 1148–1158.
- Stone, N. & Reinberg, D. (1992). Protein kinase from *Aspergillus nidulans* that phosphorylate the carboxyl-terminal domain of the largest subunit of RNA polymerase II. *J. Biol. Chem.* **267**, 6353–6360.
- Suzuki, M. (1990). The heptad repeat in the largest subunit of RNA polymerase II binds by intercalating into DNA. *Nature*, **344**, 562–565.
- Svejstrup, J. Q., Feaver, W. J., LaPointe, J. & Kornberg, R. D. (1994). RNA polymerase transcription factor IIIH holoenzyme from yeast. *J. Biol. Chem.* **269**, 28044–28045.
- Sweetser, D., Nonet, M. & Young, R. A. (1987). Prokaryotic and eukaryotic RNA polymerases have homologous core subunits. *Proc. Natl Acad. Sci. USA*, **84**, 1192–1196.
- Thompson, C. M., Koleske, A. J., Chao, D. M. & Young, R. A. (1993). A multisubunit complex associated with the RNA polymerase II CTD and TATA-binding protein in yeast. *Cell*, **73**, 1361–1375.
- Thompson, N. E., Steinberg, T. H., Aronson D. B. & Burgess, R. R. (1989). Inhibition of *in vivo* and *in vitro* transcription by monoclonal antibodies prepared against wheat germ RNA polymerase II that react with the heptapeptide repeat of eukaryotic RNA polymerase II. *J. Biol. Chem.* **264**, 11511–11520.
- Usheva, A., Maldonado, E., Goldring, A., Lu, H., Huobavi, C., Reinberg, D. & Aloni, Y. (1992). Specific interaction between the nonphosphorylated form of RNA polymerase II and the TATA-binding protein. *Cell*, **69**, 871–881.
- West, M. L. & Corden, J. L. (1995). Construction and analysis of yeast RNA polymerase II CTD deletion and substitution mutations. *Genetics*, **140**, 1223–1233.
- Wilson, I. A., Niman, H. L., Houghten, R. A., Cherenon, A. R., Connolly, M. L. & Lerner, R. A. (1984). The structure of an antigenic determinant in a protein. *Cell*, **37**, 767–778.
- Woychik, N. A. & Young, R. A. (1989). RNA polymerase II subunit RPB4 is essential for high- and low-temperature yeast cell growth. *Mol. Cell. Biol.* **9**, 2854–2859.
- Yuryev, A. & Corden, J. L. (1994). Identification of suppressors of lethal substitutions in the CTD of yeast RNA polymerase II. *J. Cell. Biochem. Suppl.* **18 part C**, 26.
- Zawel, L., Lu, H., Cisek, L. J., Corden, J. L. & Reinberg, D. (1993). The cycling of RNA polymerase II during transcription. In *Cold Spring Harbor Symposia on Quantitative Biology: DNA and Chromosomes*, pp. 187–198, Cold Spring Harbor Laboratory Press, Plainview, NY.
- Zhang, J. & Corden, J. L. (1991a). Identification of phosphorylation sites in the repetitive carboxyl-terminal domain of the mouse RNA polymerase II largest subunit. *J. Biol. Chem.* **266**, 2290–2296.
- Zhang, J. & Corden, J. L. (1991b). Phosphorylation causes a conformational change in the carboxyl-terminal domain of the mouse RNA polymerase II largest subunit. *J. Biol. Chem.* **266**, 2297–2302.

Edited by A. Klug

(Received 6 December 1995; received in revised form 14 February 1996; accepted 16 February 1996)